

POWER CONTROL FOR CELLULAR COMMUNICATIONS WITH TIME-VARYING CHANNEL UNCERTAINTIES

Sankrith Subramanian, John M. Shea, and Warren E. Dixon

ABSTRACT

Power control in a code-division multiple access (CDMA) based cellular network is a challenging problem because the communication channels change rapidly because of multipath fading. These rapid fluctuations cause detrimental effects on the control efforts required to regulate the signal-to-interference plus noise ratios (SINRs) to the desired level. Thus, there is a need for power-control algorithms that can adapt to rapid changes in the channel gain caused by multipath fading. Much of the previous work has either neglected the effects of fast fading, assumed that the fading is known, or assumed that all the link gains are known. In this paper, we model the effects of fast fading and develop practical strategies for robust power control based on SINR measurements in the presence of the fading. We develop a controller for the reverse link of a CDMA cellular system, and use a Lyapunov-based analysis to prove that the SINR error is globally uniformly ultimately bounded. We also utilize a linear prediction filter that utilizes local SINR measurements and estimates of the Doppler frequency that can be derived from local SINR measurements to improve the estimate of the channel fading used in the controller. The power-control algorithm is simulated for a cellular network with multiple cells, and the results indicate that the controller regulates the SINRs of all the mobile terminals (MTs) with low outage probability. In addition, a pulse-code-modulation technique is applied to allow the control command to be quantized for feedback to the transmitter. Simulation results indicate that the outage probabilities of all the MTs are still within the acceptable range if at least 3-bit quantization is employed. Comparisons to a standard algorithm illustrate the improved performance of the predictive controller.

Key Words: Lyapunov analysis, MMSE, power control, CDMA.

I. INTRODUCTION

Various transmitter power-control methods have been developed to deliver a desired quality of service (QoS) in wireless networks [1–9]. Early work on power control using a centralized approach was investigated in [1], which introduced the concept of signal-to-interference (SIR)-balancing, where it is desired that all receivers achieve the same SIR. Methods were developed to reduce co-channel interference for a given channel allocation using transmitter power control in [3]. In [3], the performance of optimum transmit-power algorithms are analyzed in terms of outage probabilities. These algorithms were framed with only path loss affecting the channel uncertainty. A distributed autonomous power-control algorithm was introduced in [4], where channel reuse is maximized. Optimal power control algorithms were introduced in [10–13]. In [12], an optimum power controller for multicell CDMA wireless networks was designed, where the

channel was assumed to be slowly varying without fading. Optimal power control algorithm for a Brownian motion based model was developed in [13], and stochastic power control algorithms were developed that required the measurement of interference. Optimization-based approaches that can provide features such as outage guarantees, robustness, and power minimization in the presence of fading but that require knowledge of all channel gains are presented in [7,8].

In [7–9], power control algorithms are designed for systems with radio channel uncertainties caused by mobility of the user terminals. These channel uncertainties include exponential path loss, shadowing, and multipath fading, which are modeled as random variables in the signal-to-interference plus noise ratio (SINR) measurements. A distributed power-control scheme was suggested in [9]; however, the fading process is modeled as slowly changing so that the channel gain can be accurately estimated, and practical limitations on the transmission power are not considered.

Multipath fading has the most critical effect on the design of a power-control system because of the time and amplitude scales. Multipath fading is caused by reflections in the environment, which cause multiple time-delayed versions of the transmitted signal to add together at the receiver. The time offsets cause the signals to add with different phases, and thus multipath fading can change significantly over

Manuscript received August 9, 2012; revised May 28, 2013; accepted December 21, 2013.

All authors are with the Department of Electrical and Computer Engineering, University of Florida, Gainesville, FL 32611-6250, USA.

This research is supported in part by NSF award numbers 0547448, 1217908, 0901491, 1161260, and a contract with the Air Force Research Laboratory, Munitions Directorate at Eglin AFB.

Warren Dixon is the corresponding author (e-mail: wdixon@ufl.edu).

distance scales as short as a fraction of a wavelength. For instance, for a system using the 900 MHz cellular band, the channel coherence time (the time for which the channel is essentially invariant) for a MT traveling at 48 km/hr is approximately 10 ms.

To allow the power controller to compensate for fast fading in the channel, channel prediction may be used. Linear models, referred to as autoregressive moving average process with exogenous input (ARMAX), were used in [14] for the power-control process. Hallen *et al.* focused on long-range fading prediction [15,16] based on the fact that the amplitude, frequency and phase of each multipath component vary much slower than the actual fading coefficient. The focus of this paper is to develop an SINR-based power-control algorithm that would reduce the outage probability in the radio link by predicting the power of the channel. The prediction-based power-control process is developed based on the evolution of radio-link parameters from the SINR dynamics and the available feedback SINR measurements.

In this paper, the radio channel characteristics discussed above are analyzed, and the fading power is predicted and used in the control design. For this purpose, a linear minimum mean-square error (LMMSE) predictor is used to obtain a reliable prediction of the fading coefficient at the next instance. In our preliminary efforts in [17], we modeled the dynamics of the stochastic time-varying radio channel for cellular radio and developed a robust power control algorithm. In our follow-up work in [18], we refined this model and introduced a predictor for the fading process. The limitation of [18] is that the predictor used measurements of the fading process, while in practice, only the SINR can be measured directly. To address this issue, a LMMSE predictor is developed in this paper that uses only SINR measurements and estimates of the Doppler frequency that can be derived from local SINR measurements, inclusive of path loss and shadowing. The motivation behind using the SINR measurements alone is that it is not possible to calculate the fading power from the SINR measurements when the latter is affected by shadowing, path loss, and interference in addition to fast fading. A Lyapunov-based analysis is performed to provide an ultimate bound on the SINR error, the size of which can be reduced by choosing appropriate control gains. In addition, variations in other components of the radio channel such as path loss and log-normal shadowing are also accounted for using this analysis tool. The controller uses local SINR measurements [4,19] from the current and neighboring cells to maintain the SINRs of MTs in the acceptable communication range, provided channel gains are limited to some practical region of operation. The real channel gains may be arbitrarily low, in which case no power control algorithm can achieve the desired performance due to limits on the available power. In these cases, the controller may not be able to regulate the SINR into the desired range,

and outage may occur, where the SINR falls too low for acceptable communication. Simulation is used to assess the performance of the proposed prediction and power-control algorithm. Other contributions of this paper over [17,18] include investigating the effects of the prediction window size and quantization on the outage performance and a performance comparison with Song's up-down power control algorithm [20].

II. NETWORK MODEL AND PROPERTIES

We consider the reverse link of a cellular system employing CDMA. The SINR $x_i(l) \in \mathbb{R}$ is defined (in dB) for each radio link $i = 1, 2, \dots, n$, as

$$x_i(l) = 10 \log \left(\frac{ag_i(l)P_i(l)}{I_i(l)} \right), \quad (1)$$

where $l \in \mathbb{Z}$, the function $\log(\cdot)$ denotes the base 10 logarithm, $g_i(l) \in \mathbb{R}$ is the channel gain in the radio link between MT i and the base station (BS), $P_i(l) \in \mathbb{R}$ is the power transmitted by MT i to the BS, $a \in \mathbb{R}$ is the bandwidth spreading factor or the processing gain [21] defined as the ratio of the transmission bandwidth (in Hertz) to the data rate (in bits/second), and $I_i(l) \in \mathbb{R}$ is the interference from the MTs in all the cells, defined as

$$I_i(l) = \sum_{j \neq i} g_j(l)P_j(l) + \eta_i. \quad (2)$$

In (2), $\eta_i \in \mathbb{R}$ denotes the thermal noise power in link i , which is assumed to be a constant value greater than zero. Since the noise power is bounded and the interference power from each MT is less than its transmit power, $I_i(\cdot)$ is non-zero and bounded.

The channel gain $g_i(l)$ in (1) is modeled as [22]

$$g_i(l) = g_{d_0} \left(\frac{d_i(l)}{d_0} \right)^{-\kappa} 10^{0.1\delta_i(l)} |H_i(l)|^2. \quad (3)$$

In (3), $g_{d_0} \in \mathbb{R}$ is the near-field gain (see [23] for model details). The second factor in (3) is the exponential path loss, which depends on the distance $d_i(l) \in \mathbb{R}$ from MT i to the BS and the path-loss exponent, $\kappa \in \mathbb{R}$, which typically takes values between two and five. Exponential path loss holds in a region outside the near-field region (*i.e.*, the region satisfying $d_f \leq d_0 \leq d_i(l)$, where d_f is the Fraunhofer distance). MTs cannot travel within distance d_0 of the BS and only communicate with the BS if they are within a predetermined radius of coverage, so $d_i(\cdot)$ is non-zero and bounded within a particular operating cell. The factors $10^{0.1\delta_i(l)}$ and $|H_i(l)|^2$ in (3) are used to model large-scale log-normal shadowing (from buildings, terrain, or foliage) and small-scale multipath fading, respectively.

For analytical purposes, the shadowing is generally modeled as log-normal; *i.e.*, $\delta_i(l) \in \mathbb{R}$ is a Gaussian random process. The fading is often modeled as Rayleigh fading, where $H_i(t)$ is usually taken to be a zero-mean, complex-valued, wide-sense stationary Gaussian random process [23], and thus $|H_i(t)|$ is a Rayleigh random variable for each t . However, both of these processes are unbounded, which means that any non-negative channel gain is possible, and hence any received power level is possible. However, $g_i(l)$ cannot take arbitrarily large values in practice because the received power cannot exceed the transmitted power. Furthermore, a cellular system cannot practically transmit to overfaded users who are in very deep fades (*i.e.*, when $g_i(l)$ is close to zero) because doing so would require extremely large power at that user and the other users (because the power transmitted to each user causes interference at the other users) [24]. Hence, the subsequent control-system development is based on the assumption that the shadowing gain $10^{0.1\delta_i(l)}$ and fading gain $|H_i(\cdot)|^2$ are both bounded from above and below. However, the performance is simulated in Section VI and Section VII for channels that may result in arbitrarily low signal levels, which may result in the power-control algorithm failing to regulate the SINR to the desired region.

Understanding how the SINR changes is beneficial for the development and analysis of the subsequent power-control law. The SINR at the next update interval $x_i(l+1) \in \mathbb{R}$ can then be expressed by taking the first difference of (1) as

$$x_i(l+1) = \varrho_i[g_i(l+1), I_i(l+1)] - \varrho_i[g_i(l), I_i(l)] + x_i(l) + u_i(l), \quad (4)$$

where the functional $\varrho_i \in \mathbb{R}$ is defined $\forall i = 1, 2, \dots, n$ as $\varrho_i(y_i, z_i) = 10 \log\left(\frac{ay_i}{z_i}\right)$, and $u_i(l) \in \mathbb{R}$ denotes an auxiliary control signal defined $\forall i = 1, 2, \dots, n$ as

$$u_i(l) \triangleq 10[\log(P_i(l+1)) - \log(P_i(l))], \quad (5)$$

which is used to determine the power update law.

III. LINEAR PREDICTION

The development of a power controller for radio links in a CDMA network is challenging due to rapid, large scale changes in SINR and is exacerbated by a constraint that each link's transmit power is less than some $P_{\max} \in \mathbb{R}$. In this paper, we attempt to improve performance by estimating the SINR $ag_i(l+1)/I_i(l+1)$ to compensate for the delays in measurement and control. Note that the various channel components that contribute to the SINR, such as fading and shadowing power and path loss are not computable from the received SINR, which motivates our design based on the SINR.

Let $X_i(\cdot) \triangleq g_i(l)/I_i(l)$. We use linear minimum mean-square error (LMMSE) prediction of $X_i(l)$ given n_1 past values, $X_i(l-1), X_i(l-2), \dots, X_i(l-n_1)$. The LMMSE estimator is [25]

$$\hat{X}_i(l) = \sum_{m=l-n_1}^{l-1} \beta_i^{(m)} \{X_i(m) - \mu\} + \mu \quad (6)$$

where the coefficients $\beta_i^{(m)}$ depend on the second-order statistics of $X_i(l)$, μ is the mean of the random process $X_i(\cdot)$ for all l . Let $f_i \triangleq \frac{v_i}{\lambda} \cos \theta_i$ be the Doppler frequency of MT i , where v_i is the velocity of motion of the MT, θ_i is the angle between the transmitted signal and the direction of motion of the MT, and λ is the wavelength of the transmitted signal. The Doppler frequency of the MT can be estimated from the SINR measurements (cf. [26]). Let T_p be the prediction observation sampling time, and the prediction observation sampling rate is selected such that it is at least the Nyquist rate, *i.e.*, twice the expected maximum of the Doppler frequencies of the MTs [16]. The coefficients $\beta_i^{(m)}$ in (6) can be determined using the orthogonality condition [25], and by using the autocovariance function for fading defined in [27,28] (we assume that the interference during the duration of the prediction sampling is approximately constant [29]). The autocovariance function for $|H_i(\cdot)|^2$ is $R_{|H_i|^2}(T_p) \approx J_0^2(2\pi f_n(T_p))$ [27,28], where J_0 is the zeroth-order Bessel function of the first kind, and f_n is the maximum Doppler frequency. Therefore, defining $\beta_i \triangleq [\beta_i^{(l-(n_1-1))}, \dots, \beta_i^{(l)}]$ and using the orthogonality condition yields

$$\beta_i^T = \begin{bmatrix} J_0^2(2\pi f_n(T_p, n_1)) \\ J_0^2(2\pi f_n(T_p, (n_1 - 1))) \\ \vdots \\ J_0^2(2\pi f_n T_p) \end{bmatrix} Z^{-1}, \quad (7)$$

where the components of Z are defined $\forall j, k = 1, 2, \dots, n_1$ as

$$Z_{jk} = Z_{kj} = \begin{cases} J_0^2(2\pi f_n(T_p, |j-k|)); & j \neq k \\ \sigma_{|H_i|^2}; & j = k, \end{cases} \quad (8)$$

$f_n \neq 0$ and $\sigma_{|H_i|^2}$ is the variance of the random process $|H_i(\cdot)|^2$ for all l . The Doppler frequency of each MT is measured periodically and this is used to update the coefficients of the LMMSE estimator. Note that the coefficients of β_i in (7) are bounded if the covariance matrix in (8) is invertible, which will occur with probability 1 if $1/T_p$ is greater than the Nyquist rate [16] and the effect of measurement noise is considered. Thus, the linear predictor $\hat{X}_i(\cdot)$ is bounded.

IV. CONTROL DEVELOPMENT

4.1 Control objective

The network QoS can be quantified by the ability of the SINR to remain within a specified operating range with upper and lower limits, $\gamma_{\min}, \gamma_{\max} \in \mathbb{R}$ for each link defined $\forall i = 1, 2, \dots, n$ as

$$\gamma_{i,\min} \leq x_i(l) \leq \gamma_{i,\max}, \quad (9)$$

where $\gamma_{i,\min}$ and $\gamma_{i,\max}$ depend on the quality-of-service requirements of mobile station i . Keeping the SINR above the minimum threshold eliminates signal dropout, whereas remaining below the upper threshold minimizes interference to adjacent cells. The control objective for the following development is to regulate the SINR to a target value $\gamma_i \in \mathbb{R}$ such that $\gamma_{i,\min} \leq \gamma_i \leq \gamma_{i,\max}$, while ensuring that the SINR remains between the specified lower and upper limits for each channel. To quantify this objective, a regulation error $e_i(l) \in \mathbb{R}$ is defined as

$$e_i(l) = x_i(l) - \gamma_i, \quad \forall i = 1, 2, \dots, n. \quad (10)$$

4.2 Closed-loop error system

By taking the first difference of (10), using (3), and (4), and properties of the $\log(\cdot)$ function, the open-loop error dynamics for each link can be determined as

$$\Delta e_i(l) = \chi_{gi}(l+1) - \chi_{gi}(l) + u_i(l), \quad (11)$$

where the auxiliary function $\chi_{gi}(\cdot) \in \mathbb{R}$ is defined $\forall i = 1, 2, \dots, n$ as

$$\chi_{gi}(\cdot) = x_i(\cdot) - 10 \log(aP_i(\cdot)) \quad (12)$$

where $\sqrt{\sum_{i=1}^n \chi_{gi}^2(\cdot)}$ is bounded based on the explanation in Section II.

Based on (11) and the subsequent stability analysis, the auxiliary power controller $u_i(l)$ is designed as

$$u_i(l) = -(k_p + k_e)e_i(l) - \hat{Y}_i(l+1) + \chi_{gi}(l), \quad (13)$$

where $\hat{Y}_i(l+1) \in \mathbb{R}$ is defined $\forall i = 1, 2, \dots, n$ as

$$\hat{Y}_i(l+1) = 10 \log \left\{ \left[\hat{X}_i(l+1) \right] \right\}, \quad (14)$$

and

$$\left| \hat{X}_i(\cdot) \right| \neq 0, \quad (15)$$

where $\hat{X}_i(\cdot)$ are given in (6), and the prediction observation sampling rate is chosen to be at least the Nyquist rate for (15)

to hold. From (5), (13), and (14), the power update law for each radio channel is obtained $\forall i = 1, 2, \dots, n$ as

$$[P_i(l+1)]_{dB} = -(k_p + k_e)e_i(l) - 10 \log \left\{ a \left[\hat{X}_i(l+1) \right] \right\} + x_i(l). \quad (16)$$

V. STABILITY ANALYSIS

Theorem I. The power update law in (16) ensures that all closed loop signals are bounded, and that the SINR regulation error approaches an ultimate bound $\varepsilon \in \mathbb{R}$, which can be decreased with increasing k_p in (13) up to the maximum power limits and decreasing the sampling intervals up to practical limits, provided k_e in (13) is selected as

$$0 < k_e \leq 1, \quad (17)$$

and γ_{\min} and γ_{\max} in (9) are chosen appropriately.

Proof. Let $V(e, l) : D \times [0, \infty) \rightarrow \mathbb{R}$ be a positive definite function defined as

$$V(e, l) = \sum_{i=1}^n \frac{1}{2} e_i^2(l). \quad (18)$$

Taking the first difference of (18), by using the fact that $\Delta(ab) = a\Delta b + b\Delta a + \Delta a\Delta b$, and substituting for (11) yields

$$\Delta V = \sum_{i=1}^n \left\{ e_i(l) [\chi_{gi}(l+1) - \chi_{gi}(l) + u_i(l)] + \frac{\Delta e_i^2(l)}{2} \right\}, \quad (19)$$

where $\Delta e_i(l)$ is the error between the sampling time for radio link i , and $\left\{ \sum_{i=1}^n \Delta e_i^2(l) \right\} / 2$ is bounded by a constant c , the size of which can be controlled by the sampling time. An analysis for this claim can be developed as in [17], though the subsequent simulation is carried out by selecting a high (and feasible) sampling rate. Substituting (13) into (19) yields

$$\Delta V \leq \sum_{i=1}^n \left\{ -k_e e_i^2(l) + e_i(l) (\chi_{gi}(l+1) - \hat{Y}_i(l+1)) - k_p e_i^2(l) \right\} + c. \quad (20)$$

by completing the squares and using (18), the inequality in (20) can be rewritten as

$$\Delta V \leq -2k_e V + \frac{\varsigma}{4k_p} + c, \quad (21)$$

where $\varsigma = \sum_{i=1}^n (\chi_{gi}(l+1) - \hat{Y}_i(l+1))^2$ is upper bounded by some positive scalar c_2 , *i.e.*, $\varsigma \leq c_2$ based on the development in Section II and Section III. Note that k_p is used to damp out $\sum_{i=1}^n (\chi_{gi}(l+1) - \hat{Y}_i(l+1))^2$ in (21) while k_e is the proportional

gain used by the controller where $0 < 2k_e \leq 1$. Provided the sufficient condition in (17) is satisfied, lemma 13.1 of [30] can be invoked, and further (18) can be used to develop an upper bound for the SINR error as

$$\sum_{i=1}^n e_i^2(l) \leq \sum_{i=1}^n e_i^2(l_0)(1-2k_e)^l + \left(\frac{1-(1-2k_e)^l}{k_e} \right) \left[\frac{c_2}{4k_p} + c \right]. \quad (22)$$

The assumption that $\chi_{gi}(l) \in \mathcal{L}_\infty$, the fact that $\hat{y}_i(l) \in \mathcal{L}_\infty$ from Section III, (14), and (15), and the fact that $e_i(l) \in \mathcal{L}_\infty$ from (22) can be used to conclude that $u_i(l) \in \mathcal{L}_\infty$ from (13), and hence $P_i(l+1) \in \mathcal{L}_\infty$ from (16). Based on (22), as $l \rightarrow \infty$, the norm-squared SINR error is ultimately bounded as $\varepsilon \leq c_2/(4k_e k_p) + c/k_e$. The ultimate bound can be decreased by increasing k_p ; however, the magnitude of k_p is practically restricted by the constraint that $0 < P_{\min} \leq P_i(t) \leq P_{\max}$, and the sampling interval T_s .

Based on the power constraint, the stability of the system is guaranteed if the given SINR thresholds γ_{\min} and γ_{\max} satisfy the following conditions: $\gamma_{\min} \leq \chi_{g\min} + [P_{\max}]_{dB}$, and $\gamma_{\max} \geq \chi_{g\max} + [P_{\min}]_{dB}$, where $\chi_{g\min} \leq |\chi_{gi}(t)| \leq \chi_{g\max}$, $\forall i$ from (12) and the explanation in Section II.

The controller is designed based on the stability analysis, that in-turn uses the nonlinear SINR model defined in (4). The bounds on the stochastic uncertainties may be high, and hence high control gains might be required to stabilize the system. Given limited available power, the SINR may go outside the thresholds of γ_{\min} and γ_{\max} . To validate the performance and hence address the feasibility of the controller, a metric known as Outage Probability, defined as the probability that the SINR $x_i(l)$ goes below γ_{\min} (i.e., $x_i(l) \leq \gamma_{\min}$), is used. Note that if $x_i(l) \geq \gamma_{\max}$, the radio link achieves better performance (lower error rates) for radio i but might increase the interference to other links. Detailed simulations in Section VI and Section VII evaluate the performance in terms of outage probabilities.

VI. SIMULATION RESULTS

A cellular network topology using the proposed power-control algorithm was simulated with one cell of interest and one tier of six adjacent cells in the typical seven-cell reuse pattern. Ten MTs were simulated in each cell. The Random-Waypoint model is used to simulate the mobility of the MTs, with the initial topology drawn from the steady state (stationary) distribution (cf. [31,32]). The mobile velocity at each waypoint is randomly chosen from a uniform distribution between 2 km/h and 48 km/h. Thus, the probability density function of the velocity is given by [32] $f_i(v) = \frac{C_h}{v} f_{v|h}^0(v)$, where $f_{v|h}^0(v) = \frac{1}{48 \text{ km/h} - 2 \text{ km/h}} = \frac{1}{46 \text{ km/h}}$ and $C_h =$

14.47 is a normalization constant. The subscript h is used to denote the phase of the MT [32]. The velocity for each of the MTs is obtained using the inverse transform method [33] as

$$v = \exp(3.179r + 0.6931), \quad (23)$$

where r is uniformly distributed between 0 and 1. The purpose of the simulation section is to detail the performance of the controller, and this is done by including the plot of the worst-case scenario of the radio-link, i.e., when the Doppler frequency is high (refer to Fig. 1). The simulations were repeated 10 times (Monte Carlo Simulations) operating 70 MTs (10 MTs in each of the typical seven-cell reuse pattern) in each simulation so that the data collected for the subsequent analysis is sufficient. Also, each simulation was carried out with fixed control gains k_p and k_e . The average value of the outage probabilities of the MTs operating in each of the four maximum Doppler frequency ranges are tabulated (refer to Table I) along with the feasible window size for various ranges of the Doppler frequencies.

Path loss, with free space propagation effects and log-normal shadowing, is modeled [23] as shown in (3). The angle θ is measured periodically, and the Doppler frequency is obtained from (23), which is used to generate the Rayleigh fading and update the coefficients of the LMMSE predictor. The channel sampling time (T_s) and prediction observation sampling time (T_p) are both set to 1.7 ms, based on performing a continuous time SINR error analysis [17]. The target SINR, γ was set to 8 dB, with a desired operating range between 6 and 10 dB, which is defined in Section 4.1. Thermal noise, η , was set to -83 dBm. The initial power level for all MTs was chosen as 10 dBm. Also, the prediction window size is updated online to avoid an ill-conditioned matrix Z . Starting at a specified maximum prediction window size, the size of the window is consecutively reduced by 1 until $\det Z \geq 10^{-5}$.

The results in Fig. 1 are obtained with $k_p = 0.65$, $k_e = 1.3 \times 10^{-4}$, and the spreading factor a is chosen as 512, which is the maximum for Wideband CDMA systems. Note that the same values of the control gains and spreading factor are also used in the subsequent simulations. The control gains were tuned using simulations with a different set of random seeds than those used in the performance evaluation. The output of the linear predictor is limited to $\hat{X}_{\max} = 47$ dB for the reasons explained in Section III.

Fig. 1 shows the SINR error, channel gain and power plots of an MT operating with a maximum Doppler frequency of 31.60 Hz. A Doppler frequency of 31.60 Hz represents an MT with high mobility. (MTs with higher velocities can rely on time diversity, rather than fading, to operate in a fading channel.) The dotted lines note the regions of deep fades, which result in large prediction errors. The inaccuracy of the linear predictor and the limits on maximum transmit power

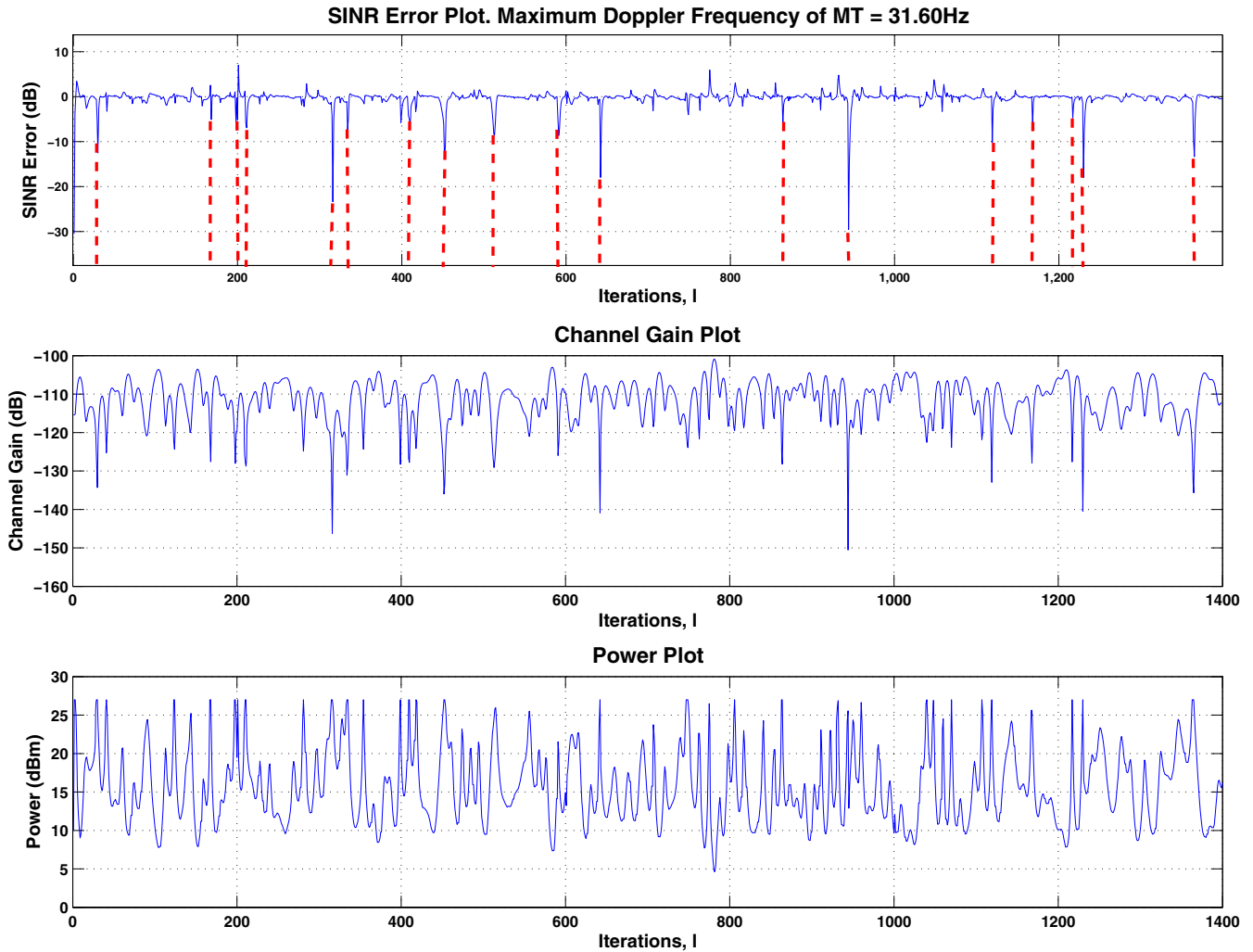


Fig. 1. Error, channel gain, and power plot of a MT with maximum Doppler frequency 31.60 Hz.

Table I. Comparison against various prediction window sizes.

Max. Doppler frequency range (Hz)	Best window size such that $\det Z \geq \zeta$	Average % of samples such that $x_i \leq \gamma_{\min}$			
		Max. Prediction window size of 1	Max. Prediction window size of 2	Max. Prediction window size of 3	Max. Prediction window size of 4
0–10	2	10.62	5.19	—	—
10–20	2, 3	15.62	4.01	6.91	—
20–30	3	19.94	13.42	7.29	—
30–40	3, 4	22.98	9.88	7.00	5.07

(and, correspondingly, control effort) in the deep faded zones cause outage at the MT at those times. The SINR of this radio link operating with a maximum Doppler frequency of 31.60 Hz is in the acceptable communication range at all other times, and the required power is in the implementable range.

Simulations were carried out for prediction-based power-control algorithms with different prediction window

sizes based on the same topology model with ten MTs in a cell to compare the results. Table I shows the average % outages for different ranges of the maximum doppler frequency (cf. [7,34]) of the MTs when the simulation is carried out using different prediction window sizes. The average % outages for the MTs were computed by running 5–10 simulations and classifying the MTs based on their maximum doppler frequencies (column 1 in Table I). The best window

Table II. Percentage of sample times experiencing outage for different number of users in the cell of interest. The control gain k_p is tuned for the system based on the number of users, and $k_e = 1.3 \times 10^{-4}$. The prediction window sizes are selected based on the condition $\det Z \geq \zeta$ (refer to Table I for the best window size selection).

Doppler freq. range (Hz)	Avg. % samples where $x_i \leq \gamma_{\min}$		
	10 users	20 users	40 users
0–10	1.3	2.2	2.6
10–20	2.1	4.1	5.0
20–30	5.1	6.1	6.7
30–40	5.5	8.4	9.5
Best k_p	0.65	0.7	1
Avg. Transmit Power (dBm)	-16.47	-15.51	-14.75

size is the maximum value of the window size so that the matrix Z is not ill-conditioned (*i.e.*, $\det Z \geq \zeta$), and the corresponding average % outage is entered in bold. The maximum doppler frequency is measured frequently (*cf.* [26] and the references therein), *i.e.*, $400T_s$ in this simulation, and the measured values are used to calculate the linear coefficients β_i^m , $\forall m = 1, 2, \dots, n_1 - 1$. It can be inferred that these bolded values fall within the threshold level for voice communications. For voice communications, the typical outage target is 10% [35].

The results in Table II show the performance of the predictive control algorithm for different numbers of users per cell. Outage probabilities less than 10% can be achieved for 10, 20, or 40 users per cell. However, the control gain k_p must be increased as the number of users to achieve this outage probability, and this results in an increase in the average transmitted power per user.

VII. QUANTIZED POWER-CONTROL

In practice, the number of bits that can be sent for power updates to the mobile terminal is limited. Thus, this section considers the design of a power-control mechanism that selects from a finite set of power adjustments. Various results in the literature focus on developing quantized power-control algorithms [6,14,36]. A power-control algorithm with a fixed step size was introduced in [6]. Due to the time-varying nature of the radio channel, the performance of this mechanism is limited. A pulse-code-modulation realization was developed in [36] to reduce the outage probability by varying the range of the power updates. In this section, a power-update mechanism based on the pulse-code-modulation realization is used to update the transmitter power at the mobile terminal, and the outage probabilities of the radio links are compared with the outage probabilities without quantization obtained in Section VI.

Table III. Percentage of sample times experiencing outage for unquantized, 2-bit and 3-bit power-control commands.

Doppler freq. range (Hz)	Avg. % samples where $x_i \leq \gamma_{\min}$		
	Unquantized	3-bit	2-bit
0–10	1.3	1.4	1.5
10–20	2.1	2.7	3.8
20–30	5.1	7.3	11.5
30–40	5.5	9.8	13.6

The realization of the power-control command is based on the error signal generated at the BS. The quantization of the error signal is done by analyzing the probability density function of the worst case unquantized error signals (*cf.* Section VI), *i.e.*, the radio links operating at the high Doppler frequency.

We assume that a power control command is only issued if the error signal is large. The presence of a power control command is usually signaled by a separate control bit (as in IS-95/cdma2000). Thus, for k -bit quantization, $2^k + 1$ levels can be used, where one level maps to a zero command. The error is then quantized by partitioning the empirical density of the error signals that operate at high maximum Doppler frequencies that are obtained from a separate simulation of the unquantized system (to avoid over-training), into bins of equal probability. The quantized value of the corresponding control is then defined as the median given that the signal lies in that bin, as that is found to offer better performance than other measures, such as the conditional mean. The quantization scheme depends on the number of bits used for quantization. The thresholds on the error when no power control command is issued is tuned (to ± 0.035 dB, in this case) based on repeated simulation of the unquantized system, quantizing the control signal, simulation of the quantized system, and performance analysis in terms of outage probability.

Monte Carlo simulations were carried out on the network topology as described in Section VI, using the 2-bit ($2^2 = 4$ combinations) and 3-bit ($2^3 = 8$ combinations) quantized error signals to determine the n -bit power control command decision that is provided to the MT. Results were obtained by first simulating using the unquantized power controller (*i.e.*, power controller with infinite feedback bandwidth). Another simulation is carried out by seeding the preceding simulation using the same random seeds, but now using a 2-bit feedback. Similarly, results are obtained for a 3-bit feedback. Then, 10 new simulations are executed using the unquantized controller, and the above mentioned process is repeated for 2-bit and 3-bit feedback. Data is collected, stored and tabulated in Table III. Table III shows the average outage probability of the various schemes (unquantized, 2-bit,

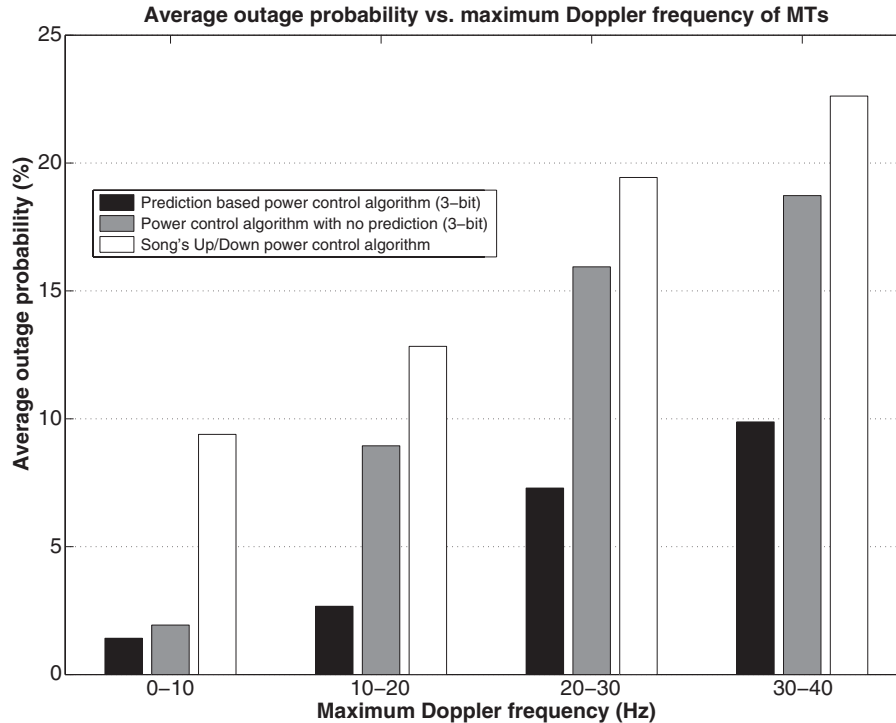


Fig. 2. Comparison against Song's power control algorithm.

and 3-bit power control command) obtained from such repeated simulations to compare and choose the best (in terms of reducing the outage probability) possible quantization scheme based on the bandwidth constraints. From Table III, a 3-bit power control command signal provides performance that falls in the acceptable region for voice communication, and hence this scheme can be used in conjunction with the controller to deliver the desired QoS for each radio link. Note that the control gains k_p and k_e are fixed throughout the course of the simulations.

We compared the performance of our control algorithm with the up/down power control algorithm described and analyzed in [20]. The up/down power control algorithm uses 1-bit feedback to determine whether to adjust the power up or down by a fixed 0.5 dB. We compare the performance of the up/down power controller to the power control algorithm developed in this paper both with and without channel prediction. The results are illustrated in Fig. 2. The results show that the use of 3-bit feedback with our control algorithm provides substantial gains over the 1-bit up/down control algorithm for all mobile velocities. For Doppler frequencies over 10 Hz, the use of channel prediction provides a significant additional performance gain, especially at high Doppler frequencies. For instance for mobile radios with Doppler frequencies between 30 Hz and 40 Hz, the up/down power controller has outage probability over 0.22. Using the power control algorithm developed in this paper, but without

channel prediction, lowers the outage probability to less than 0.19. The addition of channel prediction further lowers the outage probability to less than 0.1, thereby satisfying the typical target outage probability for mobile voice communications. The complexity of the power-control scheme proposed in this paper is dominated by the calculation of the SINR predictor in (6). This requires matrix inversion (see (7)), which has complexity that scales approximately as $\mathcal{O}(n^3)$, where n is the number of samples used in the predictor. However, the simulation results presented in this section show that $n \leq 4$ is sufficient for this purpose, and the matrix inversions need only be calculated at the rate of the channel updates. This is minimal complexity compared to the many other high-rate, low latency signal processing and decoding operations that must be carried out by the CDMA cellular base station. Thus, the proposed schemes both have the potential to improve the performance of power control in the reverse link of CDMA cellular communications and are practical for implementation in the cellular base stations.

VIII. CONCLUSION

A LMMSE prediction-based power-control algorithm was developed for a wireless CDMA-based multiple cellular networked system despite uncertain multipath fading. The predictor uses local SINR measurements at the previous and

current time instances, along with the Doppler frequency (which can also be estimated from the SINR measurements) to estimate the channel uncertainties. A Lyapunov-based analysis is used to develop the controller and a resulting ultimate bound for the sampled SINR error, which can be decreased up to a point by increasing the control gains. Simulations indicate that the SINRs of all the radio links are regulated in the region $\gamma_{\min} \leq x_i(\cdot) \leq \gamma_{\max}$ with an outage probability of less than 10%, and power requirements of all the MTs were in the implementable range. Outages at some samples were determined to be due to limitations of the linear predictor, and this highlights the need for more sophisticated prediction and control development tools to address this issue. Simulations are also done using 2-bit and 3-bit control feedback, and the results show that the performance is still within the acceptable outage range if at least a 3-bit power control command is used. Comparison against a standard power control algorithm from the literature is done to demonstrate the advantages of using channel prediction and multi-bit feedback.

REFERENCES

1. Aein, J., "Power balancing in systems employing frequency reuse," *COMSAT Tech. Rev.*, Vol. 3, pp. 277–299 (1973).
2. Alavi, H. and R. W. Nettleton, "Downstream power control for a spread spectrum cellular mobile radio system," in *Proc. IEEE Glob. Telecommun. Conf.*, Miami, Florida, pp. 84–88 (1982).
3. Zander, J., "Performance of optimum transmitter power control in cellular radio systems," *IEEE Trans. Veh. Technol.*, Vol. 41, pp. 57–62 (1992).
4. Foschini, G. and Z. Miljanic, "A simple distributed autonomous power control algorithm and its convergence," *IEEE Trans. Veh. Technol.*, Vol. 42, pp. 641–646 (1993).
5. Yates, R. D., "A framework for uplink power control in cellular radio systems," *IEEE J. Sel. Areas Commun.*, Vol. 13, pp. 1341–1347 (1995).
6. Ariyavisitakul, S., "SIR-based power control in a CDMA system," in *Proc. IEEE Glob. Telecommun. Conf.*, Orlando, Florida, pp. 868–873 (1992).
7. Kandukuri, S. and S. Boyd, "Optimal power control in interference-limited fading wireless channels with outage-probability specifications," *IEEE Trans. Wirel. Commun.*, Vol. 1, No. 1, pp. 46–55 (2002).
8. Tan, C. W., "Optimal power control in rayleigh-fading heterogeneous networks," in *Proc. 2011 IEEE INFOCOM*, Shanghai, China, pp. 2552–2560 (2011).
9. Jagannathan, S., M. Zawodniok, and Q. Shang, "Distributed power control for cellular networks in the presence of channel uncertainties," *IEEE Trans. Wirel. Commun.*, Vol. 5, No. 3, pp. 540–549 (2006).
10. Varanasi, M. and D. Das, "Fast stochastic power control algorithms for nonlinear multiuser receivers," *IEEE Trans. Commun.*, Vol. 50, No. 11, pp. 1817–1827 (2002).
11. Holliday, T., N. Bambos, P. Glynn, and A. Goldsmith, "Distributed power control for time varying wireless networks: Optimality and convergence," in *Proc. Ann. Allerton Conf. Commun. Control Computing*, Vol. 41, No. 2, pp. 1024–1033 (2003).
12. Alpcan, T., X. Fan, T. Basar, M. Arcak, and J. Wen, "Power control for multicell CDMA wireless networks: a team optimization approach," in *Int. Symp. Model. Optim. Mob. Ad Hoc Wireless Netw.*, Washington, DC, pp. 379–388 (2005).
13. Olama, M. M., S. M. Djouadi, and C. D. Charalambous, "Stochastic power control for time-varying long-term fading wireless networks," *EURASIP J. Appl. Signal Process.*, Vol. 2006, pp. 253–253 (2006).
14. Rintamaki, M., H. Koivo, and I. Hartimo, "Adaptive closed-loop power control algorithms for CDMA cellular communication systems," *IEEE Trans. Veh. Technol.*, Vol. 53, No. 6, pp. 1756–1768 (2004).
15. Eyceoz, T., A. Duel-Hallen, and H. Hallen, "Deterministic channel modeling and long range prediction of fast fading mobile radio channels," *IEEE Commun. Lett.*, Vol. 2, No. 9, pp. 254–256 (1998).
16. Duel-Hallen, A., S. Hu, and H. Hallen, "Long range prediction of fading signals: Enabling adaptive transmission for mobile radio channels," *IEEE Signal. Process. Mag.*, Vol. 17, No. 3, pp. 62–75 (2000).
17. Subramanian, S., J. Shea, and W. E. Dixon, "Power control for cellular communications with channel uncertainties," in *Proc. Am. Control Conf.*, St. Louis, Missouri, pp. 1569–1574 (2009).
18. Subramanian, S., J. Shea, and W. E. Dixon, "Prediction-based power control for distributed cellular communication networks with time-varying channel uncertainties," in *Proc. IEEE Conf. Decis. Control*, Shanghai, China, pp. 1998–2003 (2009).
19. Bambos, N., S. Chen, and G. Pottie, "Channel access algorithms with active link protection for wireless communication networks with power control," *IEEE-ACM Trans. Netw.*, Vol. 8, No. 5, pp. 583–597 (2000).
20. Song, L., N. B. Mandayam, and Z. Gajic, "Analysis of an up/down power control algorithm for the CDMA reverse link under fading," *IEEE J. Select. Commun.*, Vol. 19, No. 2, pp. 277–286 (2001).
21. Viterbi, A. J., *CDMA: Principles of Spread Spectrum Communication*, Addison Wesley, Redwood City, CA (1995).
22. Canchi, R. and Y. Akaiwa, "Performance of adaptive transmit power control in $\pi/4$ DQPSK mobile radio

systems in flat Rayleigh fading channels,” in *Proc. IEEE Veh. Technol. Conf.*, Vol. 2, pp. 1261–1265 (1999).

23. Rappaport, T., *Wireless Communications, Principles and Practice*, Prentice Hall, Upper Saddle River, NJ (1999).
24. Gao, L. and T. Wong, “Power control and spreading sequence allocation in a CDMA forward link,” *IEEE Trans. Inf. Theory*, Vol. 50, No. 1, pp. 105–124 (2004).
25. Stark, H. and J. Woods, *Probability and Random Processes with Applications to Signal Processing*, 3rd ed., Prentice Hall, Englewood Cliffs, NJ (2002).
26. Krasny, L., H. Arslan, D. Koilpillai, and S. Chennakeshu, “Doppler spread estimation in mobile radio systems,” *IEEE Commun. Lett.*, Vol. 5, No. 5, pp. 197–199 (2001).
27. Clarke, R. H., “A statistical theory of mobile-radio reception,” *Bell Sys. Tech. J.*, Vol. 47, No. 6, pp. 957–1000 (1968).
28. Jakes, W. C., *Microwave Mobile Communications*, Wiley, New York (1974).
29. Qian, L. and Z. Gajic, “Variance minimization stochastic power control in cdma systems,” *IEEE Trans. Wirel. Commun.*, Vol. 5, No. 1, pp. 193–202 (2006).
30. Spooner, J., M. Maggiore, R. Ordonez, and K. Passino, *Stable Adaptive Control and Estimation for Nonlinear Systems*, Wiley, New York (2002).
31. PalChaudhuri, S., J.-Y. Le Boudec, and M. Vojnovic, “Perfect simulations for random trip mobility models,” in *Proc. Annu. Simul. Symp.*, Washington DC, pp. 72–79 (2005).
32. Le Boudec, J.-Y. and M. Vojnovic, “Perfect simulation and stationarity of a class of mobility models,” in *Proc. IEEE Int. Conf. Comput. Commun.*, Vol. 4, pp. 2743–2754 (2005).
33. Devroye, L., *Non-Uniform Random Variate Generation*, Springer-Verlag, New York (1986).
34. Papandriopoulos, J., J. Evans, and S. Dey, “Optimal power control for Rayleigh-faded multiuser systems with outage constraints,” *IEEE Trans. Wireless Commun.*, Vol. 4, No. 6, pp. 2705–2715 (2005).
35. Suzuki, M. and H. Sasaoka, “Performance of orthogonal TPC-CDMA cellular system using cell configuration strategy,” in *Proc. Vehicle Navigation and Information Systems Conf.*, Yokohama, Japan, pp. 181–186 (1994).
36. Chang, C.-J., J.-H. Lee, and F.-C. Ren, “Design of power control mechanisms with PCM realization for the uplink of a DS-CDMA cellular mobile radio system,” *IEEE Trans. Veh. Technol.*, Vol. 45, No. 3, pp. 522–530 (1996).



Sankrith Subramanian is presently working at xG Technology, Inc., Florida. He received his Bachelor of Engineering degree in instrumentation and control engineering from St. Joseph’s College of Engineering, India, in 2006, and Master of Science degree in

electrical and computer engineering from the University of Florida in 2009. He received his Ph.D. in electrical and computer engineering, University of Florida, in 2012 and was involved with the Nonlinear Controls and Robotics group and Wireless Information Networking Group. His advisers were Dr. Warren Dixon and Dr. John Shea. He was Post-Doctoral Associate at Air Force Research Laboratory / UF-REEF at Eglin Air Force Base, FL, before joining xG Technology, Inc. His research interests lie in the field of cross-layer design in wireless networks and networked control systems.



John M. Shea (S’92-M’99) received the B.S. (with highest honors) in computer engineering from Clemson University in 1993 and the M.S. and Ph.D. degrees in electrical engineering from Clemson University in 1995 and 1998, respectively. Dr Shea is currently Associate Professor of electrical and computer engineering at the University of Florida. Prior to that, he was Assistant Professor at the University of Florida from July 1999 to August 2005 and Post-doctoral Research Fellow at Clemson University from January 1999 to August 1999. He was Research Assistant in the Wireless Communications Program at Clemson University from 1993 to 1998. He is currently engaged in research on wireless and military communications. Dr. Shea received the Technical Achievement Award for contributions to military communications from the IEEE Military Communications Conference (MILCOM) in 2012. He received the Eilersick Award from the IEEE Communications Society for the Best Paper in the Unclassified Program of MILCOM in 2013 and 1996. He received the Outstanding Young Alumni award from the Clemson University College of Engineering and Science in 2011. He was selected as a Finalist for the 2004 Eta Kappa Nu Outstanding Young Electrical Engineer. Dr. Shea has been Editor for IEEE Wireless Communications magazine since 2010. He was Editor for the IEEE Transactions on Wireless Communications from 2008 to 2012 and was Associate Editor for the IEEE Transactions on Vehicular Technology from 2002 to 2007. He was the Technical Program Chair for the Unclassified Program of MILCOM in 2010.



Warren Dixon received his Ph.D. in 2000 from the Department of Electrical and Computer Engineering from Clemson University. After completing his doctoral studies he was selected as Eugene P. Wigner Fellow at Oak Ridge National Laboratory (ORNL). In 2004, Dr Dixon joined the University of Florida in the Mechanical and Aerospace Engineering Department. Dr. Dixon’s main research interest has been the development and application of Lyapunov-based control techniques for uncer-

tain nonlinear systems. He has published 3 books, an edited collection, 9 chapters, and over 250 refereed journal and conference papers. His work has been recognized by the 2013 Fred Ellersick Award for Best Overall MILCOM Paper, 2012–2013 University of Florida College of Engineering Doctoral Dissertation Mentoring Award, 2011 American Society of Mechanical Engineers (ASME) Dynamics Systems and Control Division Outstanding Young Investigator Award, 2009 American Automatic Control Council (AACC) O. Hugo Schuck (Best Paper) Award, 2006 IEEE Robotics and Automation Society (RAS) Early Academic

Career Award, an NSF CAREER Award (2006–2011), 2004 DOE Outstanding Mentor Award, and the 2001 ORNL Early Career Award for Engineering Achievement. He is an IEEE Control Systems Society (CSS) Distinguished Lecturer. He currently serves as the Director of Operations for the Executive Committee of the IEEE CSS Board of Governors. He is currently or formerly Associate Editor for ASME Journal of Dynamic Systems, Measurement and Control, Automatica, IEEE Transactions on Systems Man and Cybernetics: Part B Cybernetics, and the International Journal of Robust and Nonlinear Control.